



A novel design of a sixth-order nonlinear modeling for solving engineering phenomena based on neuro intelligence algorithm

Zulqurnain Sabir¹ · Muhammad Asif Zahoor Raja² · Muhammad Shoaib³ · R. Sadat⁴ · Mohamed R. Ali^{5,6}

Received: 13 April 2021 / Accepted: 29 December 2021 / Published online: 16 January 2022
© The Author(s), under exclusive licence to Springer-Verlag London Ltd., part of Springer Nature 2022

Abstract

The current study aims to present a novel design of a sixth-order (SO) nonlinear Emden–Fowler nonlinear system (SO-NSEFM) along with its five types. The novel design of SO-NSEFM is achieved using the typical second-order Emden–Fowler system. The detail of the singularity and shape factors is presented for each type of the SO-NSEFM. Three different examples of each type of the designed SO-NSEFM will be solved using the supervised neural network (SNN) Levenberg–Marquardt backpropagation approach (LMBA), i.e., SNN–LMBA. A reference dataset using the spectral collocation scheme with the proposed SNN–LMBA will be established for the designed SO-NSEFM. The achieved approximate outcomes of the designed SO-NSEFM are accessible using the procedures of testing, verification, and training of the proposed neural networks to reduce the MSE. For the efficiency, correctness, and effectiveness of the proposed SNN–LMBA, the investigations are presented through the proportional performances of regression, MSE results, correlation and error histograms (EHs), and regression.

Keywords Sixth-order nonlinear Emden–Fowler model · Shape factors · Levenberg–Marquardt backpropagation · Spectral collocation scheme

1 Introduction

The singular systems got more importance in the last few decades due to their wider range of applications in different areas of science, technology, and engineering. The present study is related to the nonlinear Emden–Fowler (NEF) model that is singular, often considered stiff, complicated, and difficult to solve due to its harder nature. The researchers

always showed interest to solve the NEF model using different analytical and numerical approaches. The NEF model has many applications in fluid dynamics, population evolution, relativistic mechanics, the study of pattern creation, and chemical reactor system. The NEF model is a second-order singular model, mathematically written as [1–5]

$$\begin{cases} \frac{d^2u}{dx^2} + \frac{\varepsilon}{x} \frac{du}{dx} + h(x)z(u) = 0, & \varepsilon \geq 1 \\ u(0) = \xi, \quad \frac{du(0)}{dx} = 0. \end{cases} \quad (1)$$

The shape factor value is represented by ε . When $h(x) = 1$, the NEF model becomes the singular Lane–Emden model (SLE) system, mathematically given as

$$\begin{cases} \frac{d^2u}{dx^2} + \frac{\varepsilon}{x} \frac{du}{dx} + z(u) = 0, & \varepsilon \geq 1 \\ u(0) = \xi, \quad \frac{du(0)}{dx} = 0. \end{cases} \quad (2)$$

The SLE model is shown in Eq. (2) proposed by famous astrophysicists Lane and Emden. This famous historical model is used in the temperature variation modeling of a spherical gas cloud, radiative cooling, mathematical physics,

✉ Mohamed R. Ali
mohamed.reda@bhit.bu.edu.eg

¹ Department of Mathematics and Statistics, Hazara University, Mansehra, Pakistan

² Future Technology Research Center, National Yunlin University of Science and Technology, 123 University Road, Section 3, Douliou, Yunlin 64002, Taiwan, ROC

³ Department of Mathematics, COMSATS University Islamabad, Attock Campus, Attock 43600, Pakistan

⁴ Department of Mathematics, Zagazig Faculty of Engineering, Zagazig University, Zagazig, Egypt

⁵ Faculty of Engineering and Technology, Future University, Cairo, Egypt

⁶ Department of Basic Science, Faculty of Engineering at Benha, Benha University, Banha 13512, Egypt

stellar configuration, polytropic star structure in astrophysics, the cluster's galaxies modeling, and self-gravitating gas clouds [6–9]. The function $z(u)$ appears in several forms in the SLE model and always provides different forms, and $z(u) = u^m$ is the most common and popular form that has attracted the researcher community. It is observed that for $m=0$ and 1, the SLE equation is known as a linear equation; otherwise, it shows nonlinear behavior. The second kind of SLE model shows the isothermal gas sphere when $z(u) = e^u$. Furthermore, some other forms of $z(u)$ show the nonlinearity, such as $\cos u$, $\sin u$, $\cosh u$, and $\sinh u$, etc. The SLE model becomes the white-dwarf model by taking $z(u) = (u^2 - C)^{1.5}$ presented by Chandrasekhar [10]. The SLM is also implemented in physical sciences [11], dusty fluid models [12], density profile of gaseous star [13], reactions based on catalytic diffusion [14], electromagnetic theory [15], sublinear neutral term [16], classical/quantum mechanics [17], morphogenesis [18], oscillating magnetic systems [19], and isotropic continuous media [20].

The singular models are always considered stiff, grim, difficult, and challenging to handle because of the singular point. There are not so many analytic and numerical methods to solve these models. Some reported methods in the literature to handle such singular models are the Adomian decomposition approach presented by Shawagfeh et al. [21]. Romas et al. [22] established the series approach for the analytic solutions of the SLE model. Singh et al. [7] proposed a Haar wavelet collocation scheme for solving SLE model. Dizicheh et al. [23] proposed the Legendre wavelet spectral scheme for solving the SLE model. Saeed et al. [24] applied the Haar Adomian scheme for solving the nonlinear fractional SLE equation. Hashemi et al. [25] solve the SLE model using the reproduced kernel and group preserving schemes. Sabir et al. [26] designed a new third order singular functional differential model and solved by the differential transformation scheme. Bender et al. [27] presented a perturbative method to solve the singularity-based models. Nouh [28] presented the results of singular systems to solve the Pade approximation and power series schemes. The solutions of the singular models using the heuristic and swarm optimization-based techniques have been presented in these citations [29–34]. Ma [35, 36] finds N-soliton solutions and tests the Hirota N-soliton conditions using the Hirota bilinear formulation. Ma et al. [37] depend on the Hirota bilinear form, the solution of quadratic function is driven for the Hirota bilinear equation, and then, they used symbolic computation to construct the lump waves. The characteristic properties of the given lump waves are detected. The motive of this study is to investigate a novel design of the sixth-order (SO) nonlinear system of Emden–Fowler equations. SO nonlinear system of Emden–Fowler model (NSEFM), i.e., SO-NSEFM are presented and numerically investigated using the supervised neural network (SNN)

Levenberg–Marquardt backpropagation approach (LMBA), i.e., SNN-LMBA. For more than two variables, the system model using the ordinary differential equations has gotten huge significance due to its wider range of applications in the scientific and engineering applications, e.g., chemical reactor, network flow in the biological field, astrophysics, nonlinear circuits, fluid dynamics, boundary layer theory, and control theory optimization [35–46]. The novelty of the current work in the light of above stated literature is presented as

- A novel SO-NSEFM is designed based on typical and standard form of Emden–Fowler system.
- The designed sixth-order Emden–Fowler model has been numerically treated using the strength of SNN-LMBA.
- A reference dataset using the spectral collocation scheme (SCS) with the proposed SNN-LMBA will be established for the novel SO-NSEFM.
- The matching of the outcomes establishes the worth of the proposed SNN-LMBA for solving the SNN-LMBA.
- The performance of the scheme through comparative studies on correlation, error histograms (EHs), mean square error (MSE), and regression metrics provide the proposed SNN-LMBA.

The remaining paper parts are given as: The construction of the novel SO-NSEFM together is provided in Sect. 2. The novel SO-NSEFM based examples are provided in Sect. 3. The detail of the proposed SNN-LMBA, essential explanation, and solutions of the novel SO-NSEFM through SNN-LMBA is derived in Sect. 4. The final declarations and future research reports are reported in last section.

2 Construction of the novel SO-NSEFM

In this section, the structure of the novel SO-NSEFM together with the shape factors and the singularity is provided. The initial conditions (ICs) of the novel SO-NSEFM are obtained using the typical NEF model. For the derivation of the novel SO-NSEFM, the mathematical formulation is given as

$$\begin{cases} x^{-p_1} \frac{d^{a_1}}{dx^{a_1}} \left(x^{p_1} \frac{d^{a_2}}{dx^{a_2}} \right) u + h_1(x) f_1(u, v) = p(x), \\ x^{-p_2} \frac{d^{a_1}}{dx^{a_1}} \left(x^{p_2} \frac{d^{a_2}}{dx^{a_2}} \right) v + h_2(x) f_2(u, v) = q(x), \end{cases} \quad (3)$$

where p_1 and p_2 are taken as real and positive, $h_1(x)$ and $h_2(x)$ are the given function values, $p(x)$ and $q(x)$ are the forcing functions, and $f_1(u, v)$ and $f_2(u, v)$ known as the linear/nonlinear based functions of u and v . To design the novel SO-NSEFM, a_1 and a_2 must be taken as

$$a_1 + a_2 = 6, \quad a_1, a_2 \geq 1. \tag{4}$$

To satisfy the above equation, the following values are taken as:

$$a_1 = 5, \quad a_2 = 1, \tag{5}$$

$$a_1 = 4, \quad a_2 = 2, \tag{6}$$

$$a_1 = 3, \quad a_2 = 3, \tag{7}$$

$$a_1 = 2, \quad a_2 = 4, \tag{8}$$

$$a_1 = 1, \quad a_2 = 5. \tag{9}$$

The first type of the novel SO-NSEFM is obtained using the values of Eq. (5) in the system (3) and given as

$$\begin{cases} x^{-p_1} \frac{d^5}{dx^5} \left(x^{p_1} \frac{d}{dx} \right) u + h_1(x) f_1(u, v) = p(x), \\ x^{-p_2} \frac{d^5}{dx^5} \left(x^{p_2} \frac{d}{dx} \right) v + h_2(x) f_2(u, v) = q(x), \end{cases} \tag{10}$$

The simplified form of the derivatives in Eq. (10) is given as

$$\begin{cases} \frac{d^5}{dx^5} \left(x^{p_1} \frac{d}{dx} \right) u = x^{p_1} \frac{d^6 u}{dx^6} + 5p_1 x^{p_1-1} \frac{d^5 u}{dx^5} + 10p_1(p_1-1)x^{p_1-2} \frac{d^4 u}{dx^4} + 10p_1(p_1-1)(p_1-2)x^{p_1-3} \frac{d^3 u}{dx^3} \\ \quad + 5p_1(p_1-1)(p_1-2)(p_1-3)x^{p_1-4} \frac{d^2 u}{dx^2} + p_1(p_1-1)(p_1-2)(p_1-3)(p_1-4)x^{p_1-5} \frac{du}{dx}, \\ \frac{d^5}{dx^5} \left(x^{p_2} \frac{d}{dx} \right) v = x^{p_2} \frac{d^6 v}{dx^6} + 5p_2 x^{p_2-1} \frac{d^5 v}{dx^5} + 10p_2(p_2-1)x^{p_2-2} \frac{d^4 v}{dx^4} + 10p_2(p_2-1)(p_2-2)x^{p_2-3} \frac{d^3 v}{dx^3} \\ \quad + 5p_2(p_2-1)(p_2-2)(p_2-3)x^{p_2-4} \frac{d^2 v}{dx^2} + p_2(p_2-1)(p_2-2)(p_2-3)(p_2-4)x^{p_2-5} \frac{dv}{dx}, \end{cases} \tag{11}$$

The updated form of the model (11) using the above equation is written as

$$\begin{cases} \frac{d^6 u}{dx^6} + \frac{5p_1}{x} \frac{d^5 u}{dx^5} + \frac{10p_1(p_1-1)}{x^2} \frac{d^4 u}{dx^4} + \frac{10p_1(p_1-1)(p_1-2)}{x^3} \frac{d^3 u}{dx^3} + \frac{5p_1(p_1-1)(p_1-2)(p_1-3)}{x^4} \frac{d^2 u}{dx^2} + \\ \quad + \frac{p_1(p_1-1)(p_1-2)(p_1-3)(p_1-4)}{x^5} \frac{du}{dx} + h_1(x) f_1(u, v) = p(x), \\ \frac{d^6 v}{dx^6} + \frac{5p_2}{x} \frac{d^5 v}{dx^5} + \frac{10p_2(p_2-1)}{x^2} \frac{d^4 v}{dx^4} + \frac{10p_2(p_2-1)(p_2-2)}{x^3} \frac{d^3 v}{dx^3} + \frac{5p_2(p_2-1)(p_2-2)(p_2-3)}{x^4} \frac{d^2 v}{dx^2} + \\ \quad + \frac{p_2(p_2-1)(p_2-2)(p_2-3)(p_2-4)}{x^5} \frac{dv}{dx} + h_2(x) f_2(u, v) = q(x). \end{cases} \tag{12}$$

The set of the ICs of the above Eq. (12) is given as

$$\begin{cases} u(0) = I_1, \quad \frac{du(0)}{dx} = \frac{d^2 u(0)}{dx^2} = \frac{d^3 u(0)}{dx^3} = \frac{d^4 u(0)}{dx^4} = \frac{d^5 u(0)}{dx^5} = 0, \\ v(0) = I_2, \quad \frac{dv(0)}{dx} = \frac{d^2 v(0)}{dx^2} = \frac{d^3 v(0)}{dx^3} = \frac{d^4 v(0)}{dx^4} = \frac{d^5 v(0)}{dx^5} = 0. \end{cases} \tag{13}$$

The obtained model is given in Eqs. (12) and (13), which shows the multiple singularities, sixth-order form, nonlinearity, and a system of differential equations. The singular points at $x = 0$ appear five times for both the parameters u and v , respectively. The values of shape factor are $5p_1, 10p_1(p_1-1), 10p_1(p_1-1)(p_1-2), 5p_1(p_1-1)(p_1-2)(p_1-3)$ and $p_1(p_1-1)(p_1-2)(p_1-3)(p_1-4)$ for $u(x)$, whereas for the parameter $v(x)$, the shape factors are $5p_2, 10p_2(p_2-1), 10p_2(p_2-1)(p_2-2), 5p_2(p_2-1)(p_2-2)(p_2-3)$ and $p_2(p_2-1)(p_2-2)(p_2-3)(p_2-4)$, respectively. It is also observed that for $p_1 = p_2 = 1$, the 3rd, 4th, 5th, and 6th expressions vanish and the shape factor reduces to 5. For $p_1 = p_2 = 2$, the 4th, 5th, and 6th expressions vanish and shape factor reduces to 10 and 20, respectively. For $p_1 = p_2 = 3$, the 5th and 6th expressions vanish and the shape factor reduces to 15, 60, and 60, respectively. Likewise, for $p_1 = p_2 = 4$, the 6th expression vanishes and the shape factor reduces to 20, 120, 240, and 120, respectively.

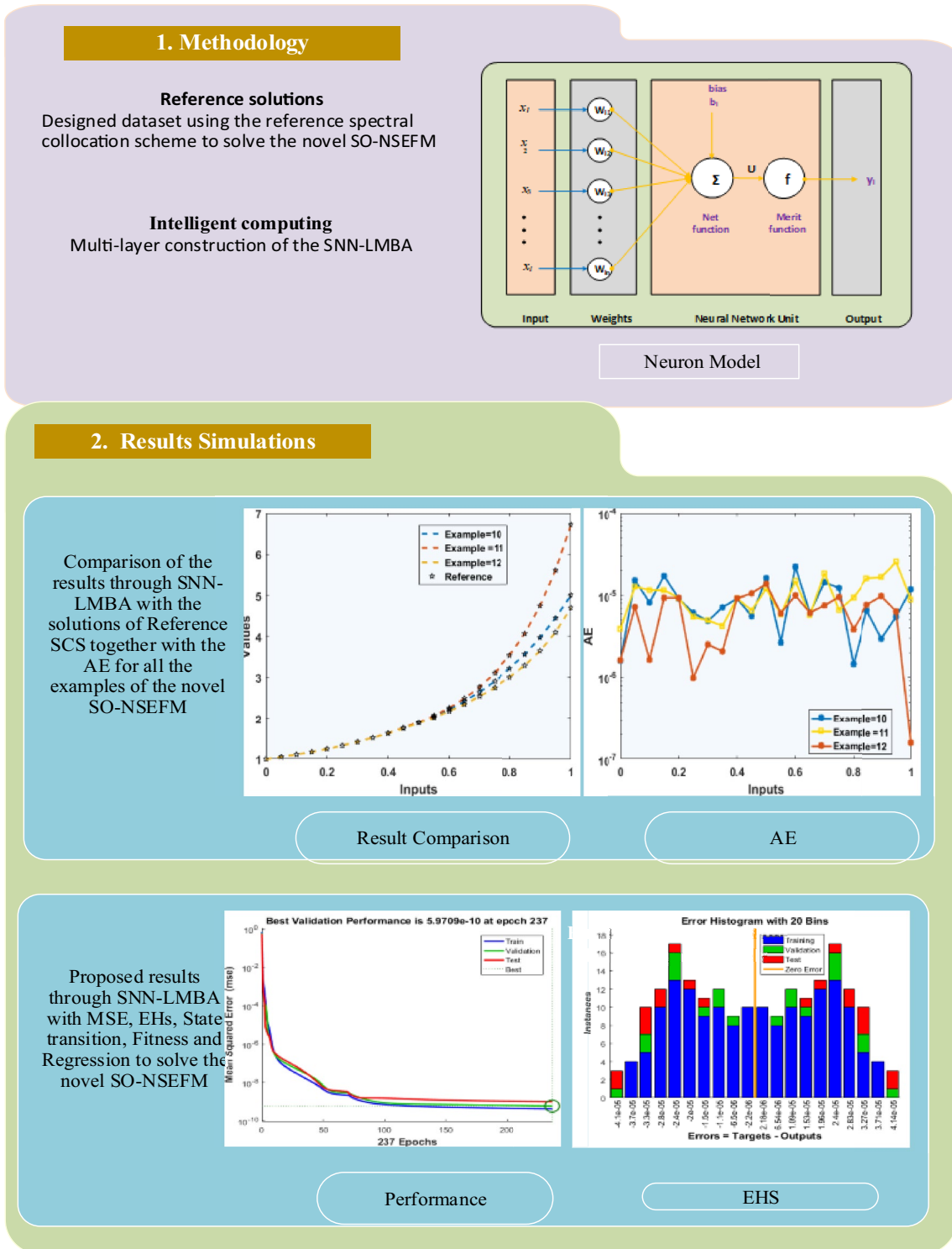
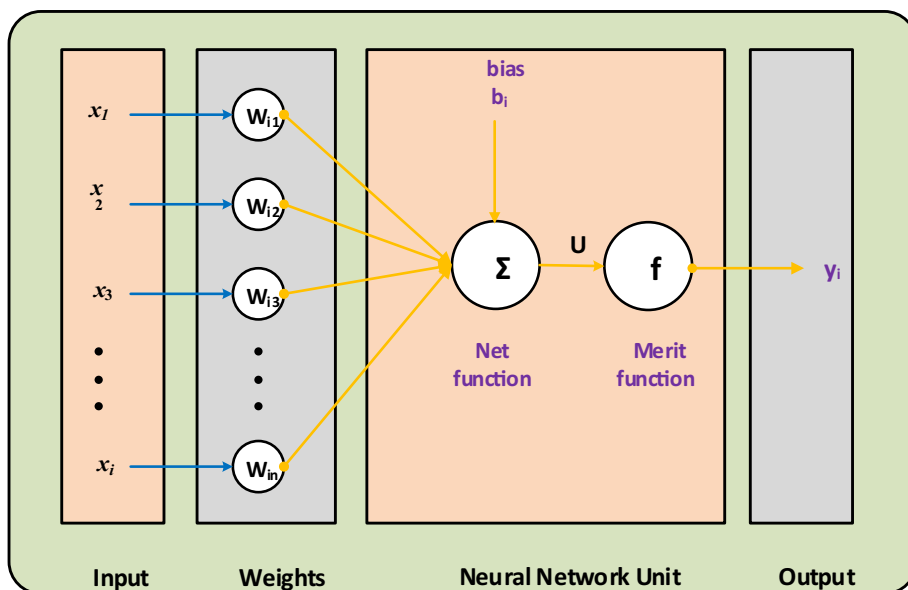


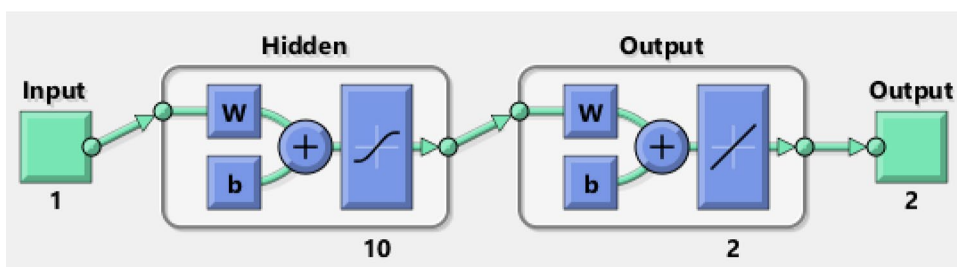
Fig. 1 Workflow diagram using the SNN-LMBA to solve the novel SO-NSEFM

Fig. 2 Designed system based on the single neuron



3 Methodology: SNN-LMBA

Fig. 3 Designed structure of the SNN-LMBA to solve the novel SO-NSEFM



4 A designed SO-NSEFM and result

The proposed scheme contains two steps: an essential explanation is provided to find the proposed SNN-LMBA dataset, while the execution process for the proposed SNN-LMBA is described (Fig. 1). The workflow diagram is represented in Fig. 2. The reference numerical results, i.e., datasets of SNN-LMBA are determined to execute the SCS. The proposed SNN-LMBA shows the multi-layer arrangements of SNNs along with LMBA. Figure 3 shows a single neuron system in SNNs scheme, while the proposed SNN-LMBA is executed using the routine of the ‘nftool’ of neural network in the MATLAB software together with the testing statics, suitably neurons setting, authentication data, learning methodology, and training data.

simulations

In this section, an example of the novel SO-NSEFM is presented. The numerical results have been provided using the designed SNN-LMBA. The achieved numerical results using the SNN-LMBA are calculated in [0, 1] interval for the novel SO-NSEFM. The designed SNN-LMBA is implemented to solve the novel SO-NSEFM using ‘nftool’ routine in the Matlab software with ten hidden neurons, training data 80%, and testing/validation data are 10% using the optimization of SNN-LMBA. The designed SNN-LMBA is provided in Fig. 3, whereas the SNN-LMBA is accomplished to solve the novel SO-NSEFM.

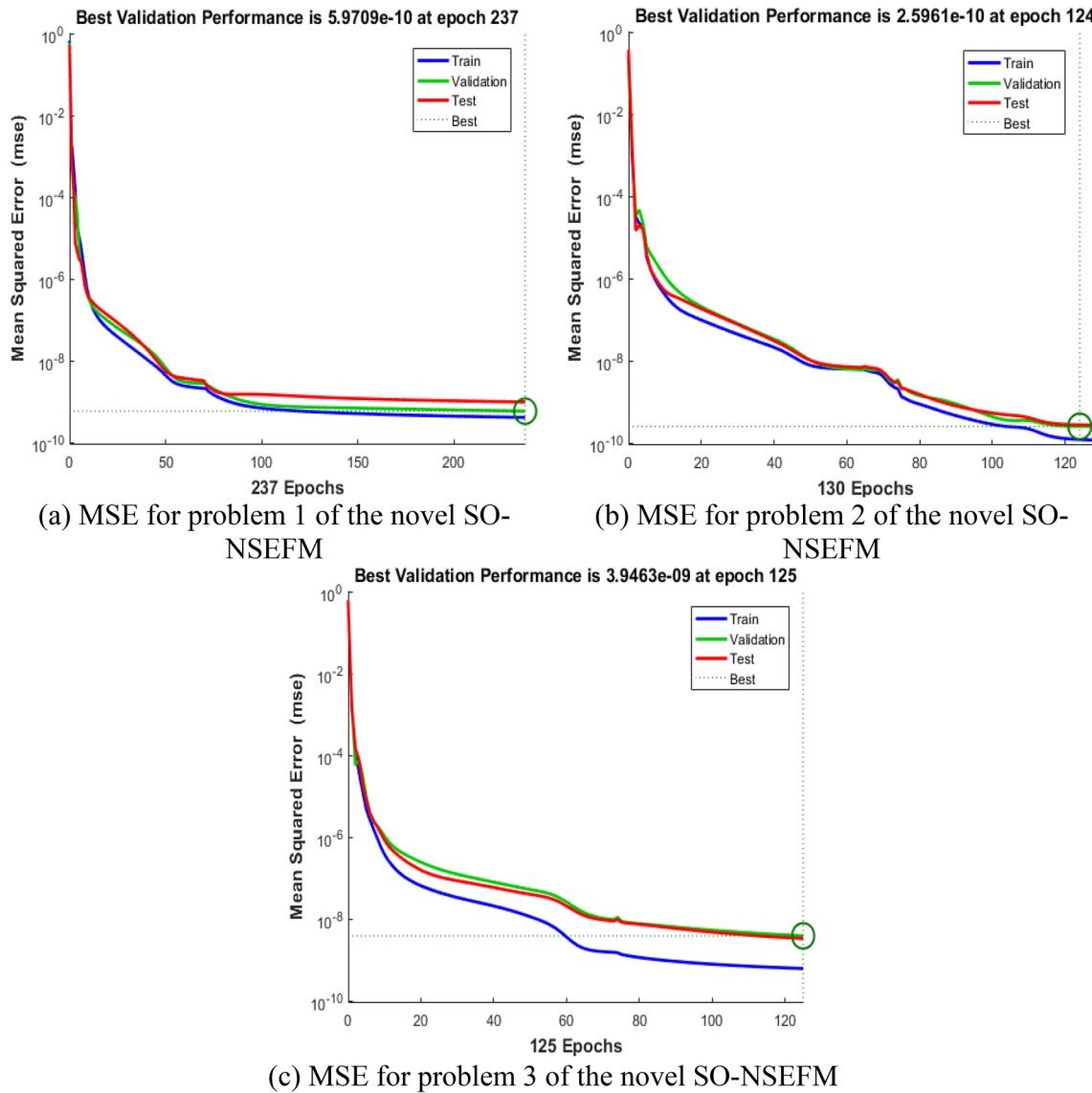


Fig. 4 Performance curves of the MSE values for the designed SNN-LMBA to solve the novel SO-NSEFM

4.1 SO-NSEFM

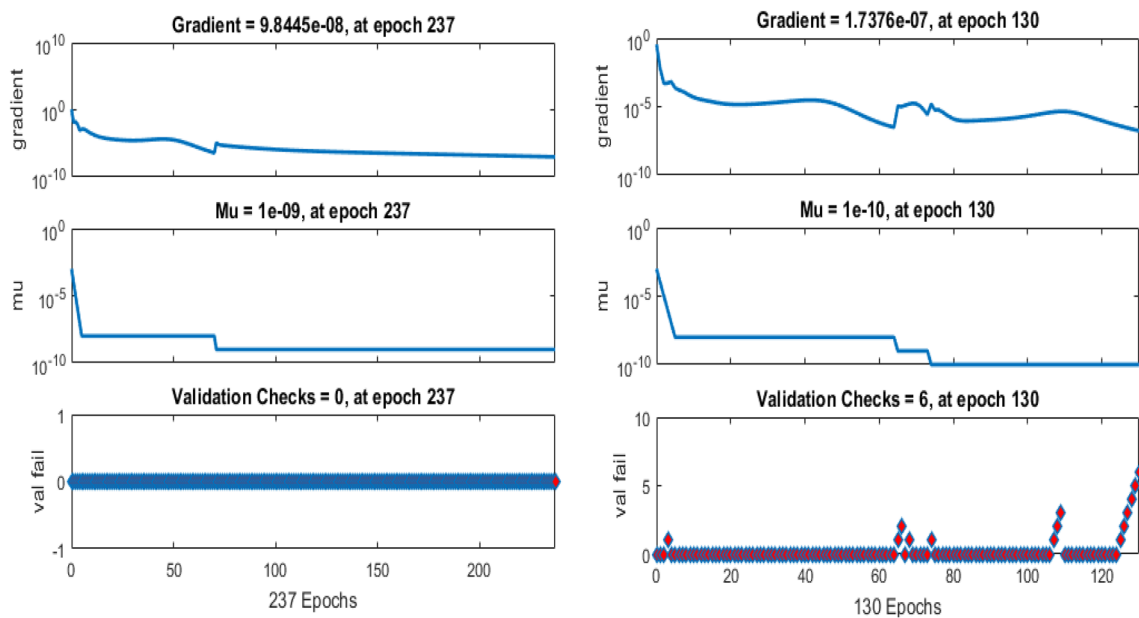
These designed model-based equations are obtained by taking the values of $p_1 = p_2 = 5$ in system (12).

Example 1: Consider

The ICs of the above model is given as

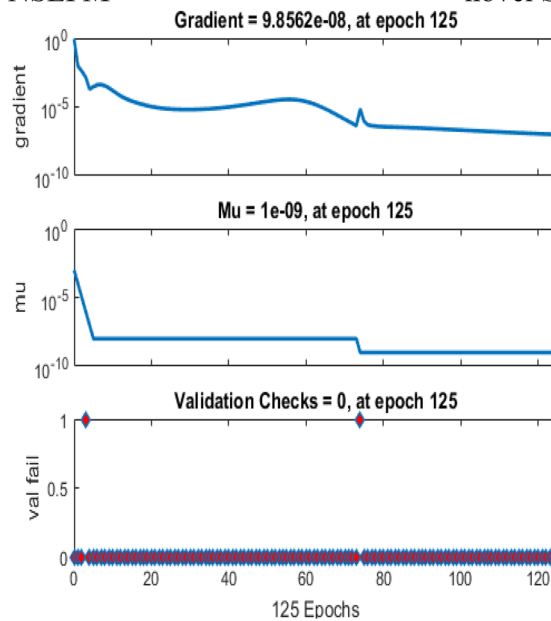
$$\begin{cases} u(0) = 1, \frac{du(0)}{dx} = \frac{d^2u(0)}{dx^2} = \frac{d^3u(0)}{dx^3} = \frac{d^4u(0)}{dx^4} = \frac{d^5u(0)}{dx^5} = 0, \\ v(0) = 1, \frac{dv(0)}{dx} = \frac{d^2v(0)}{dx^2} = \frac{d^3v(0)}{dx^3} = \frac{d^4v(0)}{dx^4} = \frac{d^5v(0)}{dx^5} = 0. \end{cases} \tag{15}$$

$$\begin{cases} \frac{d^6u}{dx^6} + \frac{25}{x} \frac{d^5u}{dx^5} + \frac{200}{x^2} \frac{d^4u}{dx^4} + \frac{600}{x^3} \frac{d^3u}{dx^3} + \frac{600}{x^4} \frac{d^2u}{dx^2} + \frac{120}{x^5} \frac{du}{dx} + u^2v = 181441 + x^6 - x^{12} - x^{18}, \\ \frac{d^6v}{dx^6} + \frac{25}{x} \frac{d^5v}{dx^5} + \frac{200}{x^2} \frac{d^4v}{dx^4} + \frac{600}{x^3} \frac{d^3v}{dx^3} + \frac{600}{x^4} \frac{d^2v}{dx^2} + \frac{120}{x^5} \frac{dv}{dx} + uv^2 = 181441 - x^6 - x^{12} + x^{18}. \end{cases} \tag{14}$$



(a) State transition for problem 1 of the novel SO-NSEFM

(b) State transition for problem 2 of the novel SO-NSEFM



(c) State transition for problem 3 of the novel SO-NSEFM

Fig. 5 State transition curves for the designed SNN-LMBA to solve the novel SO-NSEFM

The plots of the example of the novel SO-NSEFM using the proposed SNN-LMBA are provided in Figs. 4, 5, 6, 7, 8, 9, 10, 11, 12. The results of the novel SO-NSEFM-based example are provided for the performance/transition states in Figs. 4, 5. The plots of the MSE convergence using the validation, training, best curve, and testing are given

for all examples of the novel SO-NSEFM in Fig. 4. The best network performance is determined at epoch 237, 124, and 125 around 5.97×10^{-10} , 2.59×10^{-9} , and 3.94×10^{-9} , respectively. The gradient measures together are evaluated using the proposed SNN-LMBA for the example of novel SO-NSEFM are $[9.84 \times 10^{-8}, 1.37 \times 10^{-7}, 9.85 \times 10^{-8}]$

Fig. 6 Results comparison of the SNN-LMBA for Example 1 of the novel SO-NSEFM

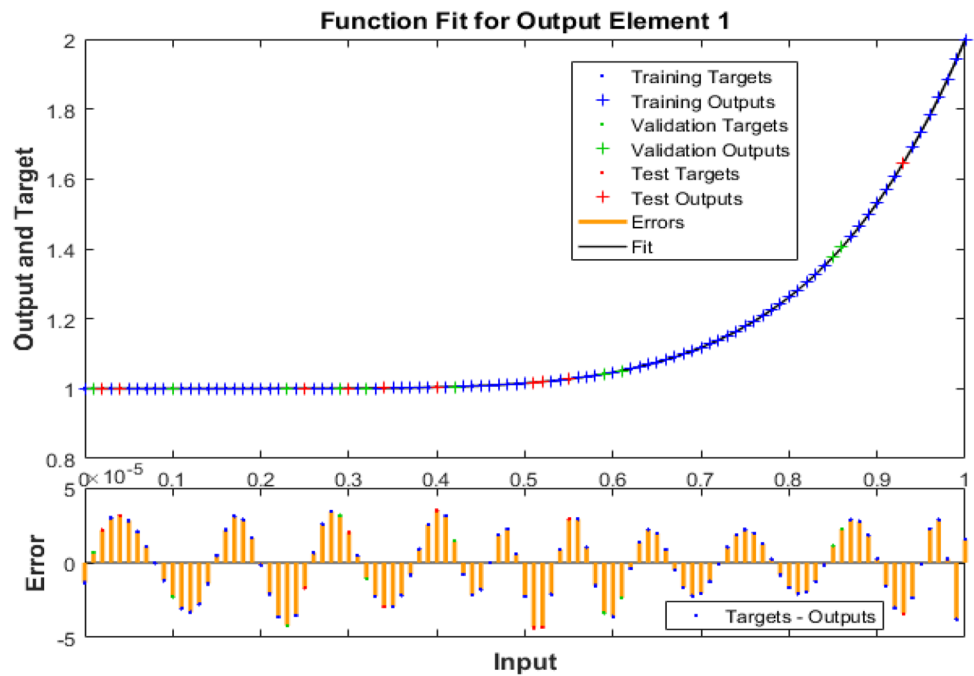
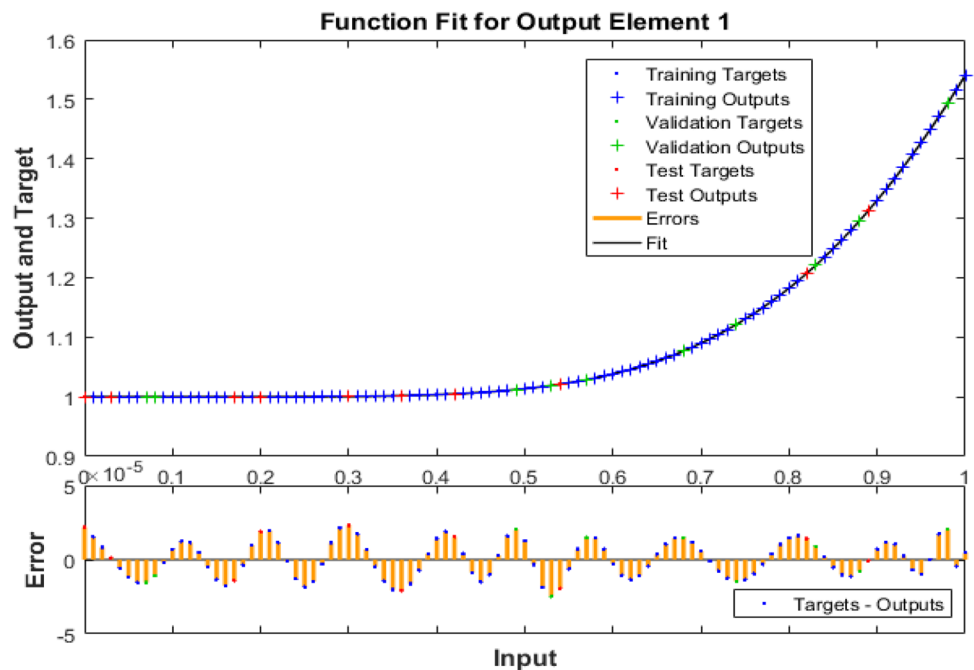


Fig. 7 Results comparison of the SNN-LMBA for Example 2 of the novel SO-NSEFM

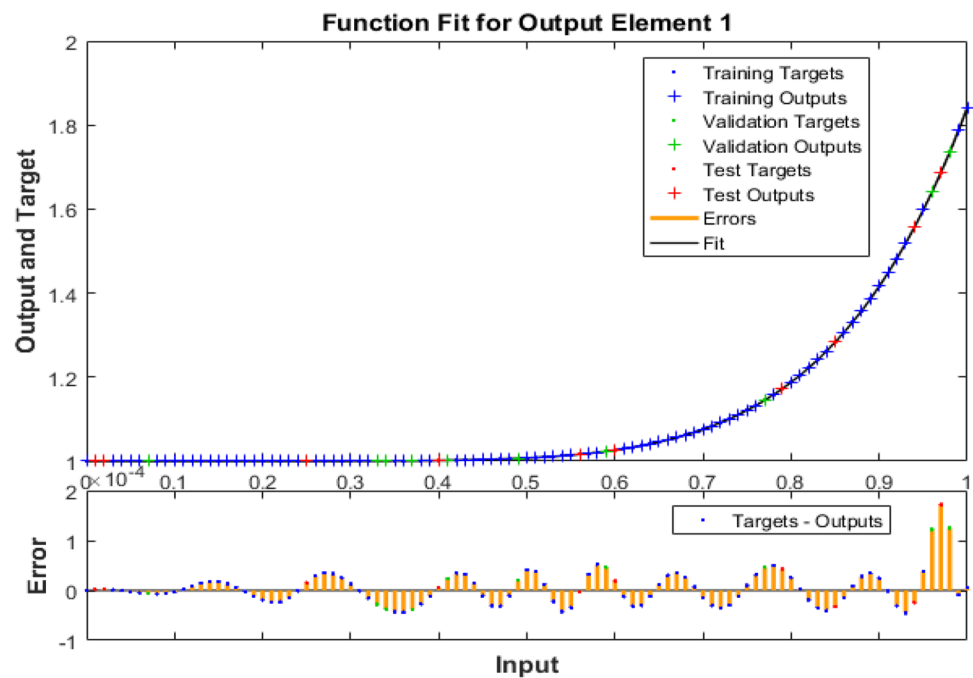


and $[1 \times 10^{-09}, 1 \times 10^{-10}, \text{ and } 9.85 \times 10^{-08}]$ and presented in Fig. 5. These values indicate the correctness and convergence of the proposed SNN-LMBA of novel SO-NSEFM.

Figures 6, 7 and 8 show the curve fitting for the example of the novel SO-NSEFM. These figures specify the comparison of the SNN-LMBA with reference solutions of the

novel SO-NSEFM together with the error plots for input span 0 to 1 using the values of the step size, i.e., 0.01. The values of maximum error for training, authentication, and testing-based proposed SNN-LMBA lie around 10^{-04} to 10^{-06} for all the example of the novel SO-NSEFM. The EH plots are presented in Fig. 9 that are used to examine the

Fig. 8 Results comparison of the SNN-LMBA for Example 3 of the novel SO-NSEFM



error investigation for the input/output intervals to solve each example of the novel SO-NSEFM. The EHs' values with zero-line reference have error lie around 2.18×10^{-06} , 1.24×10^{-06} , and 8.6×10^{-06} for the example of the novel SO-NSEFM. The plots of regression are provided in Figs. 10, 11, 12 for the example of the novel SO-NSEFM. These investigations using the correlation are performed to perform the regression investigation. It is also determined that the correlation (R) is calculated 1, which indicates the form of perfect system. This behavior shows the correctness of the proposed SNN-LMBA to solve the novel SO-NSEFM. Additionally, MSE convergence is attained through testing, performance, backpropagation procedures, validation, training, executed epochs, and complexity of time are provided in Table 1 to solve the novel SO-NSEFM.

Figures 13 and 14 show the comparison of the results obtained by the designed SNN-LMBA to solve the example using the novel SO-NSEFM. The parameter $u(x)$ and $v(x)$ results of the novel SO-NSEFM are plotted in Fig. 13a, b. The overlapping of the outcomes shows the correctness and the excellence of the designed scheme. The absolute error (AE) plots for the novel SO-NSEFM are drawn in Fig. 14. These AE values for $u(x)$ and $v(x)$ are provided in Fig. 14a, b. It is observed that the AE values for both of the parameters for $u(x)$ and $v(x)$ lie around $[10^{-04}, 10^{-06}]$ for example 1, $[10^{-04}, 10^{-05}]$ for example 2, and $[10^{-05}, 10^{-07}]$ for example 3, respectively. These

matching of the outcomes established the worth of the designed SNN-LMBA.

5 Conclusion

The present study is related to design a novel sixth-order Emden–Fowler singular nonlinear system using the typical Emden–Fowler system. Three examples of the novel model are provided together with the details of shape factors and singularities. It is seen that the first four types involve multiple singularities and shape factors, and the novel model has been designed based on the nonlinearity, logarithmic functions, exponential and trigonometric functions. The solutions of the novel sixth-order Emden–Fowler singular nonlinear system have been presented using the supervised LMBNNA. The approximation data are applied 80% for training, 10% for both testing and validation using the optimization procedure with ten hidden neurons. For the perfection of the designed model and scheme, the matching plots obtained by the designed scheme with the reference dataset are provided along with the absolute error (AE) plots. To check the mean square error, the convergence-based values for best curve, testing, training, and validation are presented for the nonlinear sixth-order Emden–Fowler singular model. The values of the correlation are provided for the regression. The values of the gradient using SNN-LMBA is evaluated for the designed

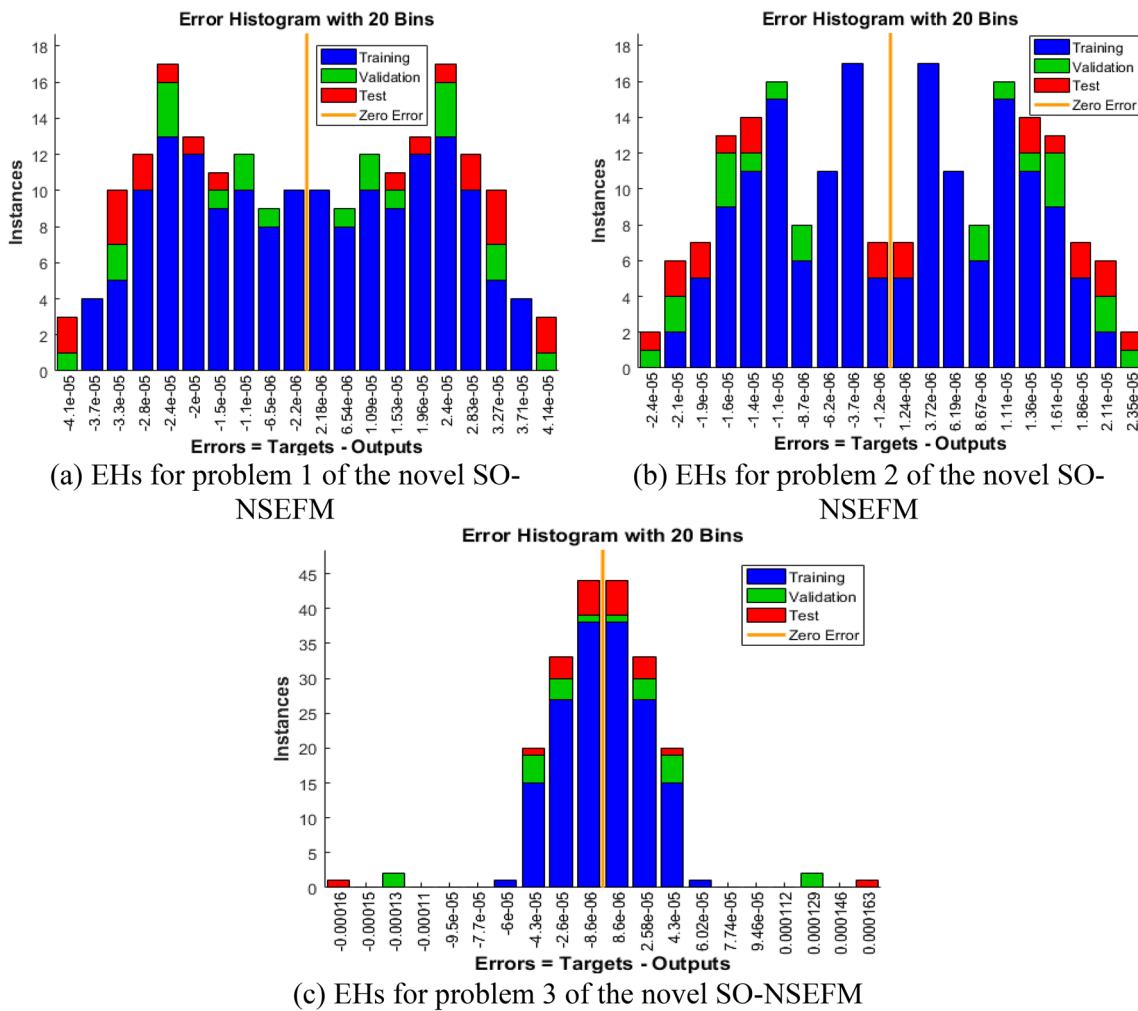


Fig. 9 EHs for the designed SNN-LMBA to solve the novel SO-NSEFM

nonlinear system. Moreover, the precision and accuracy are justified using the graphical as well as numerical illustrations of regression dynamics, error histograms, and convergence on MSE.

In future, a variety of singular, biological models, and fluid and fractional order models can be constructed and can be solved using the LMBNN [47–55].

Fig. 10 Regression performances for the designed SNN-LMBA to solve the Example 1 using the novel SO-NSEFM

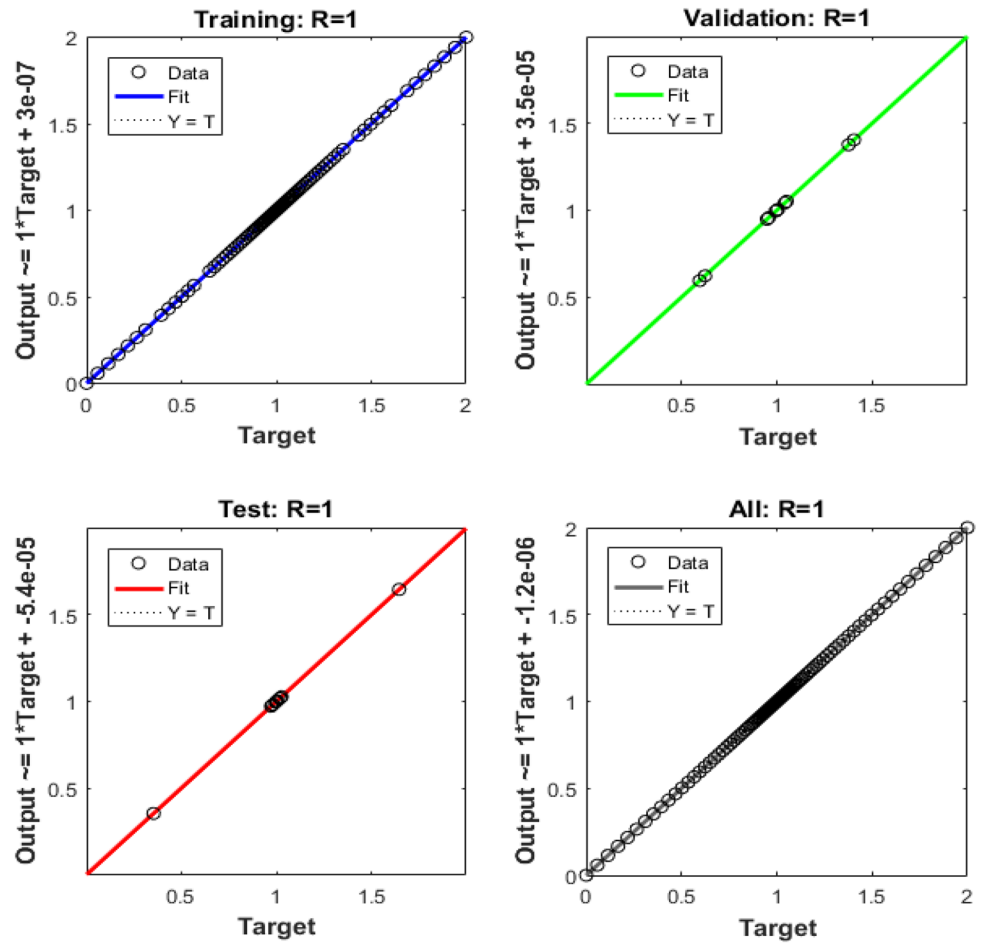


Fig. 11 Regression performances for the designed SNN-LMBA to solve the Example 2 using the novel SO-NSEFM

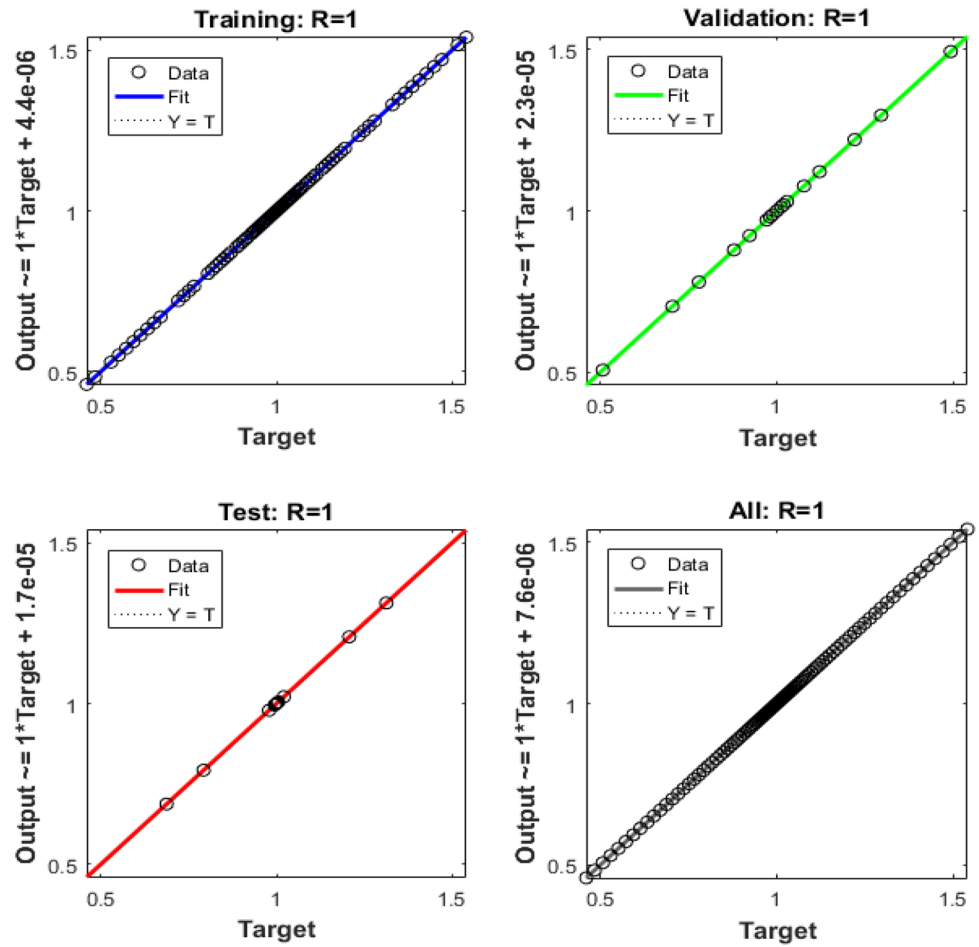


Fig. 12 Regression performances for the designed SNN-LMBA to solve the Example 3 using the novel SO-NSEFM

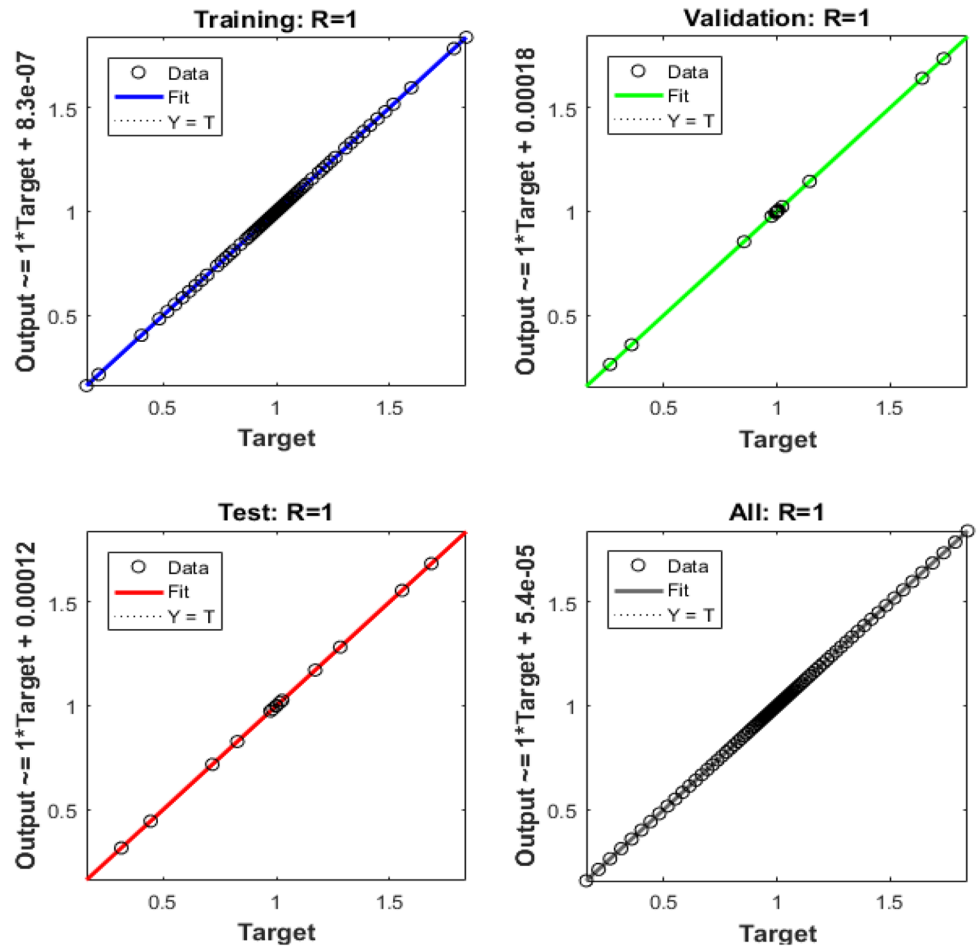


Table 1 SNN-LMBA results based on of the novel SO-NSEFM

Example	MSE			Performance	Gradient	Mu	Iteration	Time
	Training	Authentication	Testing					
1	4.19×10^{-10}	5.97×10^{-10}	1.00×10^{-09}	4.20×10^{-10}	9.84×10^{-08}	1.00×10^{-09}	237	2
2	1.24×10^{-10}	2.59×10^{-10}	2.82×10^{-10}	1.19×10^{-10}	1.74×10^{-07}	1.00×10^{-10}	130	1
3	6.28×10^{-10}	3.94×10^{-10}	8.92×10^{-10}	6.28×10^{-10}	9.86×10^{-08}	1.00×10^{-09}	125	1

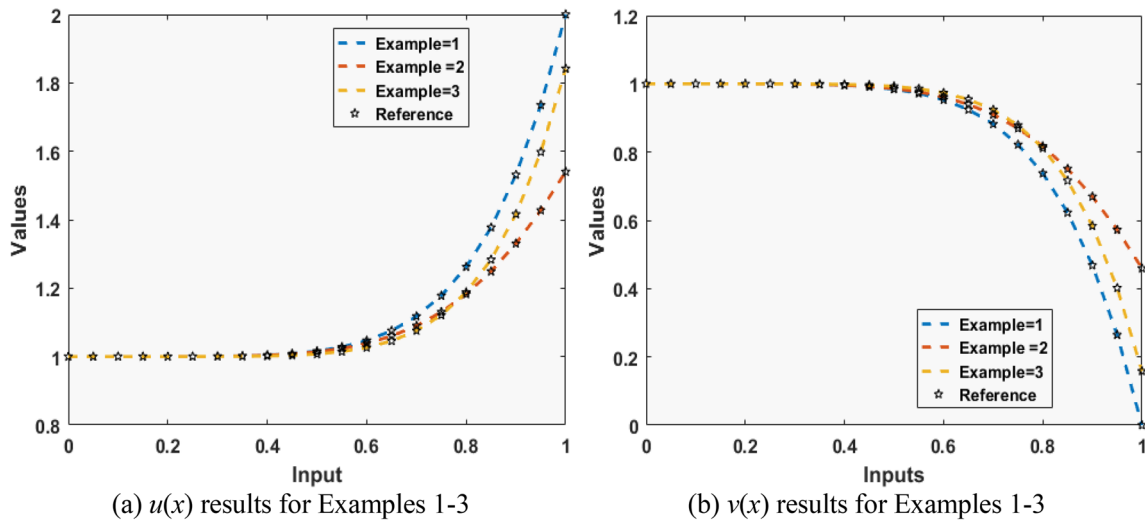


Fig. 13 Results' comparison of the designed SNN-LMBA to solve the Examples 1–3 using the novel SO-NSEFM

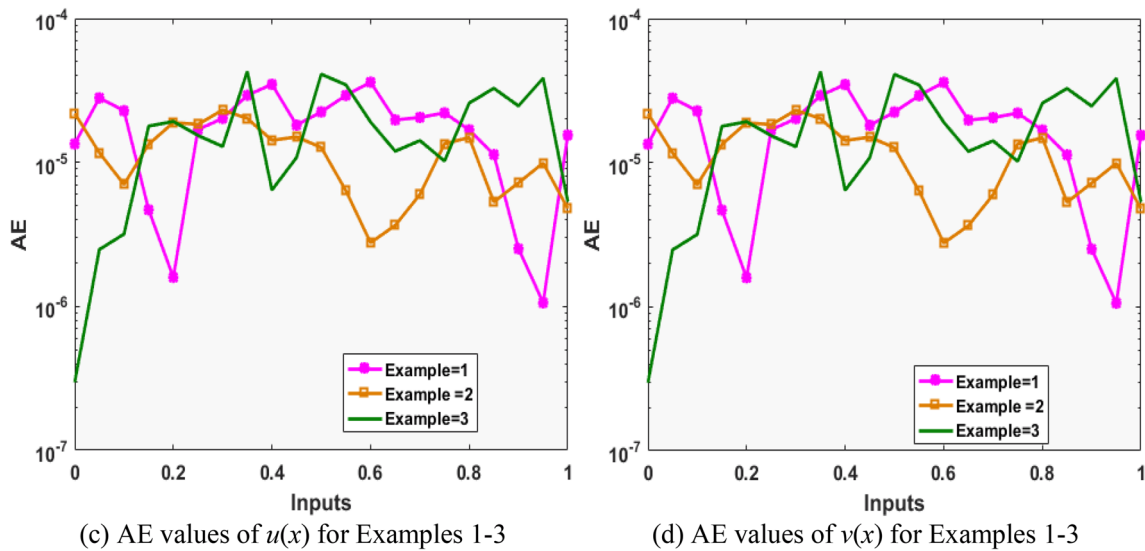


Fig. 14 Values of the AE of $u(x)$ and $v(x)$ to solve the Examples 1–3 using the novel SO-NSEFM

Declarations

Conflict of interest The authors state that they have no conflict of interest.

References

1. Sabir Z et al (2020) Novel design of Morlet wavelet neural network for solving second order Lane-Emden equation. *Math Comput Simul*
2. Adel W, Sabir Z (2020) Solving a new design of nonlinear second-order Lane-Emden pantograph delay differential model via Bernoulli collocation method. *Eur Phys J Plus* 135(6):427
3. Guirao JL, Sabir Z, Saeed T (2020) Design and numerical solutions of a novel third-order nonlinear Emden–Fowler delay differential model. *Math Probl Eng*
4. Li T, Rogovchenko YV (2017) Oscillation criteria for second-order superlinear Emden-Fowler neutral differential equations. *Monatshefte für Mathematik* 184(3):489–500
5. Sabir Z, Amin F, Pohl D, Guirao JL () Intelligence computing approach for solving second order system of Emden–Fowler model. *J Intell Fuzzy Syst* pp1–16
6. Ahmad I et al (2017) Neural network methods to solve the Lane-Emden type equations arising in thermodynamic studies of the spherical gas cloud model. *Neural Comput Appl* 28(1):929–944
7. Singh R, Shahni J, Garg H, Garg A (2019) Haar wavelet collocation approach for Lane-Emden equations arising in mathematical physics and astrophysics. *Eur Phys J Plus* 134(11):548

8. Abbas F, Kitanov P, Longo S (2019) Approximate solutions to lane-Emden equation for stellar configuration. *Appl Math Inf Sci* 13:143–152
9. Li D, Lou YQ, Esimbek J (2018) Lane-Emden equation with inertial force and general polytropic dynamic model for molecular cloud cores. *Mon Not R Astron Soc* 473(2):2441–2464
10. Chandrasekhar S (1967) An introduction to the study of stellar structure. Dover Publications, New York
11. Mandelzweig VB, Tabakin F (2001) Quasi linearization approach to nonlinear problems in physics with application to nonlinear ODEs. *Comput Phys Commun* 141(2):268–281
12. Flockerzi D, Sundmacher K (2011) On coupled Lane-Emden equations arising in dusty fluid models. In: *Journal of physics: conference series*, IOP Publishing, Vol 268(1), p 012006
13. Luo T, Xin Z, Zeng H (2016) Nonlinear asymptotic stability of the Lane-Emden solutions for the viscous gaseous star problem with degenerate density dependent viscosities. *Commun Math Phys* 347(3):657–702
14. Rach R, Duan JS, Wazwaz AM (2014) Solving coupled Lane-Emden boundary value problems in catalytic diffusion reactions by the Adomian decomposition method. *J Math Chem* 52(1):255–267
15. Khan JA et al (2015) Nature-inspired computing approach for solving non-linear singular Emden-Fowler problem arising in electromagnetic theory. *Connect Sci* 27(4):377–396
16. Div{z}urina S, Grace SR, Jadlovsk{a} I, Li T (2020) Oscillation criteria for second-order Emden–Fowler delay differential equations with a sublinear neutral term. *Math Nachr* 293:1–13. <https://doi.org/10.1002/mana.201800196>
17. Ramos JI (2003) Linearization methods in classical and quantum mechanics. *Comput Phys Commun* 153(2):199–208
18. Ghergu M, Radulescu V (2007) On a class of singular Gierer-Meinhardt systems arising in morphogenesis. *Comptes Rendus Mathématique* 344(3):163–168
19. Dehghan M, Shakeri F (2008) Solution of an integro-differential equation arising in oscillating magnetic fields using He’s homotopy perturbation method. *Progress Electromagn Res* 78:361–376
20. Radulescu V, Repovš D (2012) Combined effects in nonlinear problems arising in the study of anisotropic continuous media. *Nonlinear Anal Theory Methods Appl* 75(3):1524–1530
21. Shawagfeh NT (1993) Non-perturbative approximate solution for Lane-Emden equation. *J Math Phys* 34(9):4364–4369
22. Ramos JI (2008) Series approach to the Lane-Emden equation and comparison with the homotopy perturbation method. *Chaos Solit Fractals* 38(2):400–408
23. Dizicheh AK, Salahshour S, Ahmadian A, Baleanu D (2020) A novel algorithm based on the Legendre wavelets spectral technique for solving the Lane–Emden equations. *Appl Numer Math*
24. Saeed U (2017) Haar Adomian method for the solution of fractional nonlinear Lane-Emden type equations arising in astrophysics. *Taiwan J Math* 21(5):1175–1192
25. Hashemi MS, Akgül A, Inc M, Mustafa IS, Baleanu D (2017) Solving the Lane-Emden equation within a reproducing kernel method and group preserving scheme. *Mathematics* 5(4):77
26. Sabir Z, Günerhan H, Guirao JL (2020) On a new model based on third-order nonlinear multi singular functional differential equations. *Math Probl Eng*
27. Bender CM, Milton KA, Pinsky SS, Simmons LM Jr (1989) A new perturbative approach to nonlinear problems. *J Math Phys* 30(7):1447–1455
28. Nouh MI (2004) Accelerated power series solution of polytropic and isothermal gas spheres. *New Astron* 9(6):467–473
29. Sabir Z et al (2020) Heuristic computing technique for numerical solutions of nonlinear fourth order Emden-Fowler equation. *Math Comput Simul* 178:534–548
30. Sabir Z et al (2020) FMNEICS: fractional Meyer neuro-evolution-based intelligent computing solver for doubly singular multi-fractional order Lane-Emden system. *Comp Appl Math* 39:303. <https://doi.org/10.1007/s40314-020-01350-0>
31. Sabir Z, Ali MR, Raja MAZ et al (2021) Computational intelligence approach using Levenberg–Marquardt backpropagation neural networks to solve the fourth-order nonlinear system of Emden-Fowler model. *Eng Comput*. <https://doi.org/10.1007/s00366-021-01427-2>
32. Sabir Z et al (2020) Design of stochastic numerical solver for the solution of singular three-point second-order boundary value problems. *Neural Comput Appl* pp 1–17
33. Sabir Z, Sakar MG, Yeskindirova M, Saldir O (2020) Numerical investigations to design a novel model based on the fifth order system of Emden-Fowler equations. *Theor Appl Mech Lett* 10(5):333–342
34. Sabir Z et al (2020) Design of neuro-swarming-based heuristics to solve the third-order nonlinear multi-singular Emden-Fowler equation. *Eur Phys J Plus* 135(6):1–17
35. Ma WX (2020) N-soliton solutions and the Hirota conditions in (2+1)-dimensions. *Opt Quant Electron* 52:511. <https://doi.org/10.1007/s11082-020-02628-7>
36. Ma W-X (2021) N-soliton solutions and the Hirota conditions in (1 + 1)-dimensions. *Int J Nonlinear Sci Numer Simul*, pp 000010151520200214. <https://doi.org/10.1515/ijnsns-2020-0214>
37. Ma WX, Bai Y, Adjiri A (2021) Nonlinearity-managed lump waves in a spatial symmetric HSI model. *Eur Phys J Plus* 136:240. <https://doi.org/10.1140/epjp/s13360-021-01212-6>
38. Shah Z et al (2020) Design of neural network based intelligent computing for neumerical treatment of unsteady 3D flow of Eyring-Powell magneto-nanofluidic model. *J Mater Res Technol*
39. Umar M et al (2020) A stochastic computational intelligent solver for numerical treatment of mosquito dispersal model in a heterogeneous environment. *Eur Phys J Plus* 135(7):1–23
40. Sabir Z, Wahab HA, Guirao JL (2022) A novel design of Gudermannian function as a neural network for the singular nonlinear delayed, prediction and pantograph differential models. *Math Biosci Eng* 19(1):663–687
41. Bukhari AH et al (2020) Design of a hybrid NAR-RBFs neural network for nonlinear dusty plasma system. *Alex Eng J* 59(5):3325–3345
42. Mehmood A et al (2020) Integrated computational intelligent paradigm for nonlinear electric circuit models using neural networks, genetic algorithms and sequential quadratic programming. *Neural Comput Appl* 32(14):10337–10357
43. Raja MAZ, Manzar MA, Shah SM, Chen Y (2020) Integrated intelligence of fractional neural networks and sequential quadratic programming for Bagley–Torvik systems arising in fluid mechanics. *J Comput Nonlinear Dyn* 15(5)
44. Bukhari AH et al (2020) Fractional neuro-sequential ARFIMA-LSTM for financial market forecasting. *IEEE Access* 8:71326–71338
45. Baleanu D, Sadat R, Ali MR (2020) The method of lines for solution of the carbon nanotubes engine oil nanofluid over an unsteady rotating disk. *Eur Phys J Plus* 135:788. <https://doi.org/10.1140/epjp/s13360-020-00763-4>
46. Khan I et al (2020) Design of neural network with Levenberg-Marquardt and Bayesian regularization backpropagation for solving pantograph delay differential equations. *IEEE Access* 8:137918–137933
47. Ayub A, Sabir Z, Shah SZH, Wahab HA, Sadat R, Ali MR (2022) Effects of homogeneous-heterogeneous and Lorentz forces on 3-D radiative magnetized cross nanofluid using two rotating disks. *Int Commun Heat Mass Transf* 130:105778

48. Sánchez YG, Sabir Z, Guirao JL (2020) Design of a nonlinear SITR fractal model based on the dynamics of a novel coronavirus (COVID-19). *Fractals* 28(08):2040026
49. Guerrero Sánchez Y, Sabir Z, Günerhan H, Baskonus HM (2020) Analytical and approximate solutions of a novel nervous stomach mathematical model. *Discrete Dyn Nat Soc*
50. Mehmood A et al (2019) Integrated intelligent computing paradigm for the dynamics of micropolar fluid flow with heat transfer in a permeable walled channel. *Appl Soft Comput* 79:139–162
51. Sadat R, Agarwal P, Saleh R et al (2021) Lie symmetry analysis and invariant solutions of 3D Euler equations for axisymmetric, incompressible, and inviscid flow in the cylindrical coordinates. *Adv Differ Equ* 2021:486. <https://doi.org/10.1186/s13662-021-03637-w>
52. Shah SZH, Ayub A, Sabir Z, Adel W, Shah NA, Yook SJ (2021) Insight into the dynamics of time-dependent cross nanofluid on a melting surface subject to cubic autocatalysis. *Case Stud Thermal Eng* 27:101227
53. Ayub A, Sabir Z, Altamirano GC et al (2021) Characteristics of melting heat transport of blood with time-dependent cross-nanofluid model using Keller-Box and BVP4C method. *Eng Comput*. <https://doi.org/10.1007/s00366-021-01406-7>
54. Sabir Z, Nisar K, Raja MAZ, Haque MR, Umar M, Ibrahim AAA, Le DN (2021) IoT technology enabled heuristic model with Morlet wavelet neural network for numerical treatment of heterogeneous mosquito release ecosystem. *IEEE Access* 9:132897–132913
55. Elsonbaty A, Sabir Z, Ramaswamy R, Adel W (2021) Dynamical analysis of a novel discrete fractional SIRS model for covid-19. *Fractals* p 2140035

Publisher's Note Springer Nature remains neutral with regard to jurisdictional claims in published maps and institutional affiliations.